INTERNATIONAL JOURNAL OF CLIMATOLOGY
Int. J. Climatol. **21**: 355–369 (2001)
DOI: 10.1002/joc.612

THE RELATIONSHIP BETWEEN THE WINTERTIME NORTH ATLANTIC OSCILLATION AND BLOCKING EPISODES IN THE NORTH ATLANTIC

AMIR SHABBAR*, JIANPING HUANG and KAZ HIGUCHI
Meteorological Service of Canada, Environment Canada, Downsview, Ontario, Canada M3H 5T4

Received 22 September 1999
Revised 24 September 2000
Accepted 28 September 2000

ABSTRACT

A systematic examination of the dynamical relationship between the North Atlantic Oscillation (NAO) and atmospheric blocking episodes in the North Atlantic during winter is undertaken. Employing the blocking criteria, as defined by Tibaldi and Molteni (1990), we first establish a statistical relationship, through compositing and linear regression analysis, between the two phenomena. The results show that the frequency of blocking formations in the North Atlantic region is sensitive to the phase of the NAO. Sixty-seven percent more winter blocking days are observed during the negative than the positive phase of the NAO. The lifetime of blocking episodes is also sensitive to the phase of the NAO. When the NAO is in the negative phase, the distribution of the length of blocking varies considerably. The average length of blocking during the negative phase is about 11 days, which is nearly twice as long as the 6-day length observed during the positive phase of the NAO. The NAO accounts for about 30% of the variation in the wintertime North Atlantic blocking episodes.

We propose a conceptual model that strengthens the statistical association and offers an explanation for a dynamical connection between the occurrences of blocking and the NAO in the North Atlantic. Application of a low-order theoretical model by Charney and DeVore (1979) and an analysis of Northern Hemisphere observed surface temperature suggest that the NAO-related difference in blocking frequency and persistence are associated with changes in the zonally asymmetric thermal forcing which, to a large extent, is determined by the phase of the NAO. For the negative phase of the NAO, the distribution of the surface air temperature anomaly is the distinctive 'warm ocean/cold land' pattern related to the resonance forcing of topography and creates a dynamical environment favourable for the formation and persistence of blocks. For the positive phase of the NAO, on the other hand, the distribution of the surface air temperature anomalies is the distinctive 'cold ocean/warm land' pattern, which reduces or destroys the resonance forcing of topography and is unfavourable for the development and persistence of blocks.

KEY WORDS: atmospheric blocking; composite analysis; conceptual model; North Atlantic; North Atlantic Oscillation; quasi-geostrophic potential vorticity; regression analysis; thermal forcing

1. INTRODUCTION

In the early 1950s and again in the mid-to-late 1960s, the establishment and persistence of major atmospheric blocks, to a great extent, controlled the winter climate of the North Atlantic (Rex, 1950; Namias, 1958; Treidl *et al.*, 1981; Knox and Hay, 1985). Coincidentally with the blocking, the North Atlantic Oscillation (NAO), which is the major source of interannual variability in the area, has been in the negative phase with higher than normal heights over Iceland and lower than normal heights over the Azores. Since the early 1970s however, the NAO changed into a positive phase (Hurrell and van Loon, 1997), along with fewer occurrences of atmospheric blocking in the North Atlantic (Knox and Hay, 1985). Figure 1 clearly indicates a prominent change in the nature of both the frequency and location of blocking

* Correspondence to: Meteorological Service of Canada, 4905 Dufferin Street, Downsview, Ontario, Canada M3H 5T4; e-mail: amir.shabbar@ec.gc.ca

from 1960–1970 to 1980–1990 over the North Atlantic. In contrast, very little change is observed in atmospheric blocking over the North Pacific between the two periods. Although the NAO is the dominant mode of atmospheric variability in the North Atlantic with time scales greater than a month, compared with an average lifetime of approximately 10 days (synoptic time scale) for atmospheric blocks (Knox and Hay, 1984), the apparent relationship between the NAO and blocking in the North Atlantic raises some interesting questions, such as:

- To what extent does the low-frequency component of the NAO affect the frequency of blocking in the North Atlantic and what is the dynamical connection between these two phenomena?
- As indicated in Figure 1, why is there a marked decrease in the blocking frequency over the midlatitude North Atlantic from the periods 1960–1970 to 1980–1990? Is this change related dynamically to the change observed in the phase of the NAO over the same periods?

A thorough understanding of both the statistical and dynamical relationships between the NAO and blocking is essential in the study of North Atlantic climate variability.

The establishment, growth and decay of blocking are also of great importance for medium-range weather forecasting in midlatitudes (Shukla and Mo, 1983; Tracton, 1990). A number of studies have addressed the simulation of the complete cycle of blocks in general circulation models (GCMs) (Tibaldi and Molteni, 1990; Tibaldi *et al*., 1997). Recently, D'Andrea *et al*. (1998) used models in the Atmospheric Model Intercomparison Project (AMIP) to diagnose and compare the ability of different GCMs to simulate Northern Hemisphere midlatitude blocking. They found that the models exhibit large differences in blocking behaviour and that there is a general tendency to underestimate both the blocking frequency and the average duration of blocks. In particular, the models have problems in producing long-lived blocking episodes in the Euro-Atlantic sector.

A number of atmospheric blocking theories have been proposed (Egger, 1978; Charney and DeVore, 1979; Tung and Lindzen, 1979; Källén, 1981). Kaas and Branstator (1993) show a strong association between blocking activity in the Northern Hemisphere and anomalous zonal mean flow. They illustrate that blocking episodes correspond to times of prominent anomalies in the planetary waves. Using a linear model, they hypothesize that these anomalies could be the result of adjustment of the planetary waves to deviations in the zonal mean state. Tung and Lindzen (1979) showed that atmospheric blocking could be explained by the linear resonance of planetary scale waves with respect to surface forcing, such as continental elevation and land–sea differential heating. In the same year, Charney and DeVore (1979) proposed a multiple equilibrium theory to explain the formation of blocks. They found that both topographical and thermal forcing are necessary in order to produce two-state equilibrium solution, of which one state is a low-index flow with a strong wave component, while the other is a high-index flow

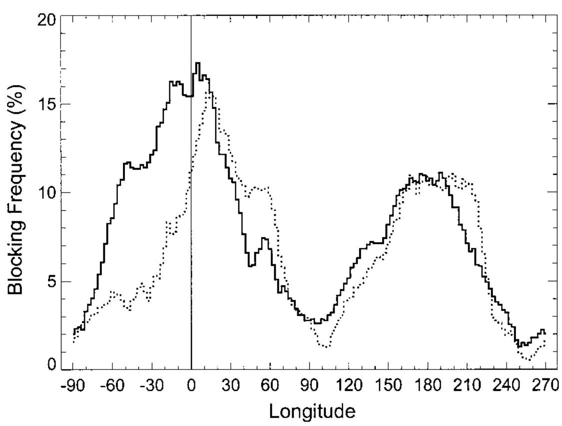

Figure 1. Decadal averaged blocking-like frequency as a function of longitude. Solid line represents the 1960–1970 average, dashed line represents 1980–1990 average

with a weak wave component. It is suggested that the phenomenon of blocking is a metastable equilibrium state of low-index with near-resonant characteristics. Interannual to interdecadal changes in the frequency of blocking formations in the North Atlantic could be related to variations in the low-index flow pattern on the same time scales. Furthermore, within the framework of the apparent association between the NAO and blocking, it is possible that the variability in the frequency of blocking formations could be related to the variations in the configuration of the surface thermal forcing through the intermediary step in which the NAO sets the stage for land–ocean thermal contrasts.

In this study, we propose a conceptual model linking the NAO, thermal forcing and blocking over the North Atlantic. The NAO is, to a great extent, responsible in determining the surface thermal configuration in the North Atlantic, eastern North America and the Euroasian sector (van Loon and Rogers, 1978a,b; Nesterov, 1998). Changes in the phase of the NAO are associated with basin-wide changes in the intensity and location of the North Atlantic jet stream and storm track. The NAO also modulates large-scale patterns of zonal and meridional heat and moisture transport (Hurrell, 1995), which in turn results in changes in temperature and precipitation patterns which often extend from eastern North America to western and central Europe (Walker and Bliss, 1932; van Loon and Rogers, 1978a,b). Changes in the surface thermal forcing induced by different phases of the NAO are then exploited in a simplified version of Charney and DeVore's (1979) theory to propose a mechanism for blocking formation in the North Atlantic sector.

Specifically in this paper, we first establish a robust statistical relationship between the phases of the NAO and the occurrence of atmospheric blocking in the North Atlantic sector. In order to provide a dynamical basis for this relationship, we invoke the concept of modulation of the surface climate by the NAO and the above-mentioned Charney/DeVore theory of thermal forcing. It is suggested that an examination of this dynamical relationship will give some insight into the possible mechanism for climate variability in the North Atlantic region.

In the next section, the data set and blocking analysis techniques used in this study are described. The statistical relationship between the NAO and blocking is presented in the following section. Along with a simplified Charney/DeVore low-order theoretical model and observed data, a discussion of the impact of the NAO on blocking frequency is presented in the section after that. In the final section, the study is concluded with a discussion of a conceptual model relating the North Atlantic atmospheric blocking to the NAO.

2. DATA AND METHODOLOGY

The data set used in this study is composed of daily averaged National Center for Environmental Prediction (NCEP) re-analysis 500 hPa height and monthly NCEP re-analysis 1000 hPa temperature data on a 2.5° by 2.5° grid, from January 1958 to December 1996 (Kalnay *et al*., 1996). Each winter, from 1958–1959 through to 1995–1996, is defined as the period beginning on 1 December and ending on 31 March of the following year.

The first NAO index was defined by Walker and Bliss (1932) as the difference between the normalized mean winter sea level pressure (SLP) anomalies at locations representative of the relative strengths of the Azores High and Icelandic Low. Rogers (1984) constructed an NAO index beginning in 1894, using SLP anomalies from Ponta Delgados, Azores and Akuyreyri, Iceland. Recently, Hurrell (1995) selected Lisbon, Portugal and Stykkisholmur, Iceland in order to extend the record another 30 years. As these NAO indices based on station pressures are affected by small-scale and transient meteorological phenomena not necessarily related to the NAO, they may contain undesirable higher frequency fluctuations. As the focus of this study is on large-scale behaviour of the North Atlantic, an NAO index based on the first rotated (varimax) empirical orthogonal function (EOF) of the 500 hPa heights is chosen. This choice of the NAO is similar to those documented by Barnston and Livezey (1987) and combines parts of the east Atlantic and west Atlantic patterns originally identified by Wallace and Gutzler (1981) for the winter season.

The NAO exhibits little variation in its climatological mean structure from month to month and consists of a north–south dipole of height and pressure anomalies, with one centre located over Greenland and the other centre of opposite sign spanning the central latitudes of the North Atlantic between 35°N and 40°N. The positive phase of the NAO reflects below-normal heights and pressure across the high latitudes of the North Atlantic and above-normal heights and pressure over the midlatitude central North Atlantic, the eastern United States and western Europe. The negative phase reflects an opposite pattern of height and pressure anomalies over these regions. In this study, the average value of the NAO index for the December to March winter period is calculated and the top (bottom) ten values are used to identify years in which the NAO remained positive (negative). These years (Table I) are then employed to investigate the behaviour of atmospheric blocking in the North Atlantic in relation to different phases of the NAO.

An objective blocking index as defined by Tibaldi and Molteni (1990), hereafter referred to as TM, is used throughout this study. The nature of the index and the criteria used in its construction are extensively discussed in TM. Here, only a brief definition is given in order to facilitate the discussion of our present study.

The 500 hPa geopotential height gradients GHGS and GHGN are computed for each longitude:

$$\mathrm{GHGS} = \frac{Z(\phi_0) - Z(\phi_s)}{\phi_0 - \phi_s} \tag{1}$$

$$\mathrm{GHGN} = \frac{Z(\phi_n) - Z(\phi_0)}{\phi_n - \phi_0} \tag{2}$$

where $\phi_n = 80°N + \Delta$, $\phi_0 = 60°N + \Delta$, $\phi_s = 40°N + \Delta$ and $\Delta = -2.5°, 0°, 2.5°$.

As the re-analysis data are on a 2.5° grid, we have chosen the spacing between latitudes to be 2.5°. TM defined their spacing to be 4°. A given longitude is defined as blocked on a specific day if both of the following conditions are satisfied (for at least one value of Δ).

$$\mathrm{GHGS} > 0$$

$$\mathrm{GHGN} < -10 \text{ m per degree latitude}$$

As described in TM, these constraints are sufficient to define a local temporal-spatial 'block-like' flow pattern, which is then used to calculate a local blocking index. The local blocking index is further constrained by imposing additional space and time constraints in order to obtain a regional blocking signature; namely, that the block-like flow pattern exists over three or more adjacent longitudes and that it lasts five days or more. We follow Tibaldi *et al.* (1997) in applying the time-continuity constraint; if a local non-block day is observed in an otherwise blocking episode of 5 consecutive days, the event is considered as a regional blocking event, with the non-blocking day assumed as a local blocking index failure. The regional blocking signature is then used to calculate distributions of such variables as blocking duration, mean blocking anomalies and monthly blocking frequency. TM definition of blocking has a built-in reason for blocking to be associated with anomalous zonal mean conditions and, therefore, one would expect a close relationship between the flow regime and block formation. However, as shown by Kaas and Branstator (1993) (KB), the relationship between blocking frequency and zonal flow is independent of the definition of blocks. KB used 15 different objective definition of blocking, including those devised by TM and found similar results between zonal mean flow and blocking frequency. The TM definition of blocking is now widely used by other investigators (e.g. D'Andrea *et al.*, 1998).

Table I. Years in which the NAO remained in the top tenth percentile (positive) and the bottom tenth percentile (negative) for the December–March period

Negative NAO	1962	1963	1964	1965	1966	1969	1970	1977	1979	1996
Positive NAO	1973	1975	1981	1983	1989	1990	1992	1993	1994	1995

These years are chosen to study the behaviour of atmospheric blocking in the North Atlantic sector. Years are labelled on January of the averaging period.

3. THE STATISTICAL RELATIONSHIP

A conceptual model which dynamically relates the NAO to blocking is developed by first establishing a clear statistical relationship between the NAO and atmospheric blocking on an interannual time scale. The interannual variability of blocking frequency in the North Atlantic region has been well documented (Lejenäs and Økland, 1983; Tibaldi and Molteni, 1990; Tibaldi *et al.*, 1997). Using the NCEP re-analysis data, we demonstrate the existence of both strong interannual and interdecadal variability in the North Atlantic region.

Figure 1 shows the decadal average of blocking-like frequency as a function of longitude. The blocking-like frequency is defined as the percentage of the number of blocking-like days per winter. No spatial or temporal constraint is yet applied. The solid line represents the average percentage frequency over the 1960–1970 period, while the dashed line is over the 1980–1990 period. Both decadal-averaged frequencies show the well-known blocking maxima, one in the North Atlantic/Europe and the other in the North Pacific. However, the change in the blocking-like frequency between the two periods is quite striking in the North Atlantic/Europe region, where there is a distinctive reduction (about 10% overall) in the blocking-like frequency (particularly over the western region) of the North Atlantic. In the North Pacific, the difference between the two decadal periods is less than 2%. These results suggest strong interdecadal variability of the blocking activity in the North Atlantic region.

Figure 1 also reflects the behaviour of the instantaneous (daily) and local (in longitude and latitude) blocking-like patterns, as no time duration and space constraints were used to calculate the blocking-like frequency. In order to diagnose the regional blocking activity, it becomes important to distinguish between instantaneous blocking-like structures and actual synoptic blocking episodes. The regional blocking frequency index, which is the blocked days per month in a given region, is calculated using the time duration constraint (5 days or more) defined in Section 2. In addition, a particular spatial sector is assumed to be blocked if three or more adjacent longitudes within its limits are defined to be blocked according to the local definition given in Section 2. Three regions of the Northern Hemisphere are studied for blocking frequency. They are:

- Canada: 130°–60°W;
- Atlantic: 60°W–10°E;
- Europe: 10°–80°E.

Wintertime blocked days in the three regions for the 1958–1996 period are depicted in Figure 2. Each time series is obtained by simply counting the number of days (5 days or greater) considered as blocked by the index for the period December–March. The North Atlantic region shows the strongest interannual variability, followed by the European region. In the North Atlantic region, the mean blocked days and the standard deviation are 31.7 and 18.2, respectively, while in the European region, the mean and the standard deviation are smaller at 13.5 and 15.2 days, respectively. To examine the linear relationship between the NAO and the regional blocking activity, correlation coefficients between the monthly NAO and the regional blocking index for the December–March period are calculated (Table II). Correlation coefficient is based on a sample size of $38 \times 4 = 152$ values (38 years and 4 months per year). The correlation coefficient between the NAO and the blocking index is -0.45 for the Canadian region and -0.54 for the North Atlantic region, with both correlation values being statistically significant at the 1% level of significance; there is no significant response in the European region. This suggests that the effect of the different phases of the NAO on blocking is localized to the North Atlantic and Canadian regions. The frequency of blocking events in these two regions tends to be higher during the winter in which the NAO is in the negative phase.

Blocking days are quantified in Figure 3 with respect to the negative (open bar) and the positive (solid bar) phases of the NAO. The composite years for the negative and positive NAO are defined in Section 2 (Table I). The frequency of wintertime blocking in the North Atlantic region is approximately 67% greater during the negative phase of the NAO than during the positive phase. During the negative phase, the average number of blocking days in the Atlantic region is 52.8, which is statistically different at the

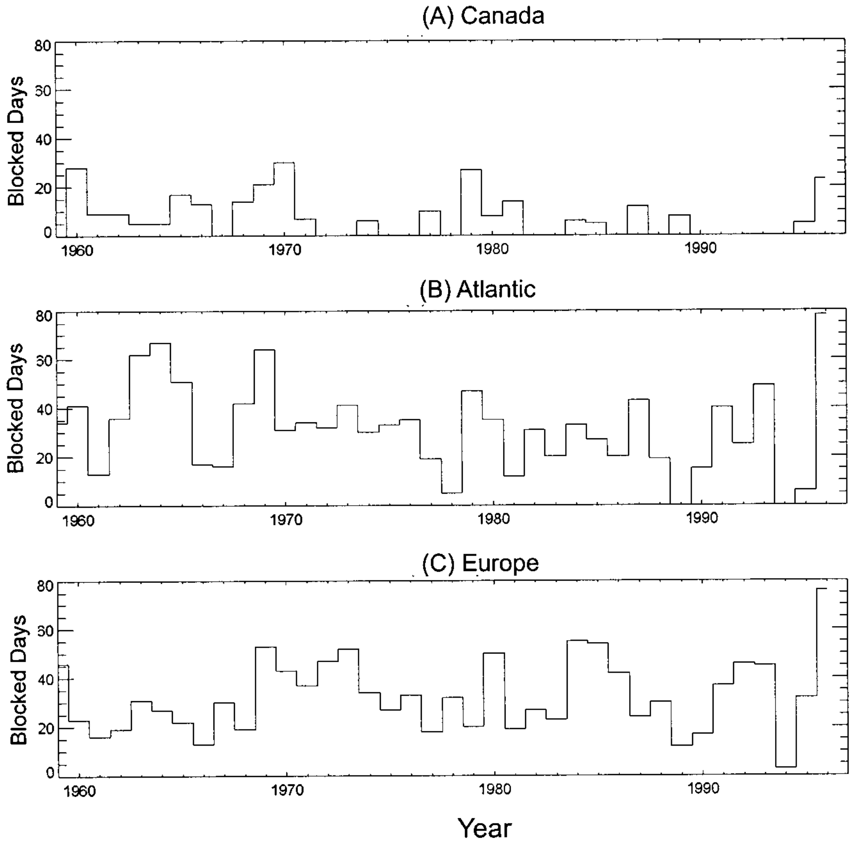

Figure 2. Time series of wintertime regional blocking days for the period 1958–1996

Table II. Correlation coefficient between monthly NAO and regional blocking index for the December–March period

Region	Canada	Atlantic	Europe
Correlation	**−0.45**	**−0.54**	0.017

Numbers in bold are statistically significant at 1%.

5% level from the climate mean of 31.7 days. For the positive phase of the NAO index, the average number of blocking days is 19.4, again statistically different from the climatic mean. The difference in blocking days from the climatic mean is also significant during the two phases of the NAO for the Canadian region. Results are similar if the composite period is changed to the months of January through March, or January through February. As the blocking events in the Canadian region are much fewer than in the North Atlantic region, we will focus our attention on the relationship between the NAO and the North Atlantic blocking.

To augment the blocking-NAO relationship that we obtained from compositing top ten and bottom ten values of the NAO index (Figure 3) regression analysis between the NAO and the North Atlantic blocking indices was carried out. Several measures of goodness-of-fit were examined. The coefficient of determination R^2, which shows the proportion of the variation of all winter blocking events that is accounted by the NAO is 0.30. As a simple regression was carried out, this implies that 30% of the variation in the North Atlantic blocking is explained by the NAO. Analysis of variance statistics indicates that the ratio

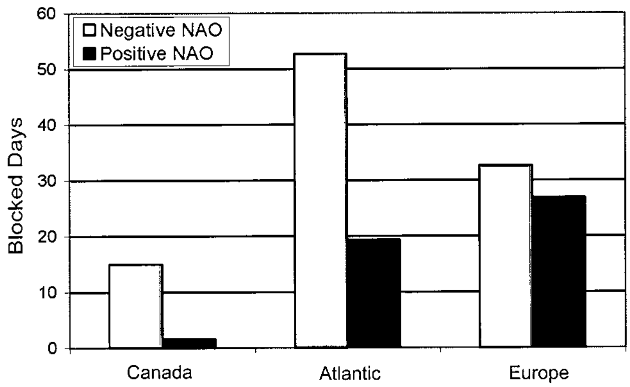

Figure 3. Composite days of regional blocking events for negative NAO (open bars) and positive NAO (solid bars). The difference between the two phases of the NAO is significant at the 5% level for the Canadian and the Atlantic regions

of mean square from the regression model to the mean square of the residual, i.e. the F-ratio of 55.5 is statistically significant at the 1% level. Moreover, an examination of the residual component of the blocking not accounted for by the NAO shows randomly distributed points about the zero line and shows no strong trends in the residual blocking behaviour. The null hypothesis of correlated residual would be rejected at the 1% level. These results indicate that the assumption of a linear relationship between the North Atlantic blocking and the NAO is a reasonable one.

Figure 4 shows the anomaly variation and its linear trend for the NAO index and the Atlantic blocking index. The NAO index shows a marked upward long-term trend, consistent with previous studies (e.g. Hurrell, 1995, 1996). It is also evident from Figure 4(B) that the Atlantic blocking index shows a systematic downward trend during the past 39 years. Note the marked change toward the negative phase of the NAO and the attendant rise in blocking days in the mid-1990s.

The frequency distribution of blocking duration for the two phases of the NAO are shown in Figure 5, suggesting a strong dependency on the phasing of the NAO. When the NAO is in the positive phase, the duration of blocking is mainly in the 5–6 day range, with more than 70% of the blocking lasting less

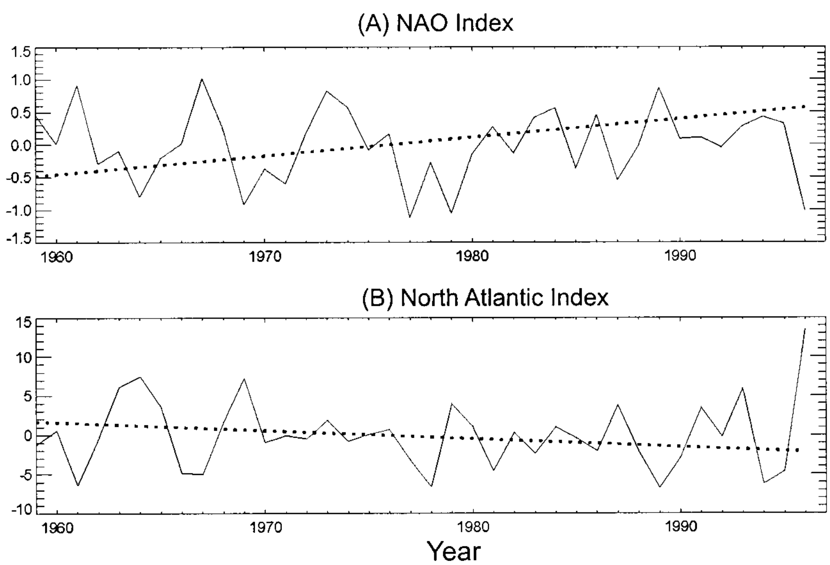

Figure 4. Anomaly variation and its long-term trend for (A) the NAO index and (B) blocking index for the Atlantic region

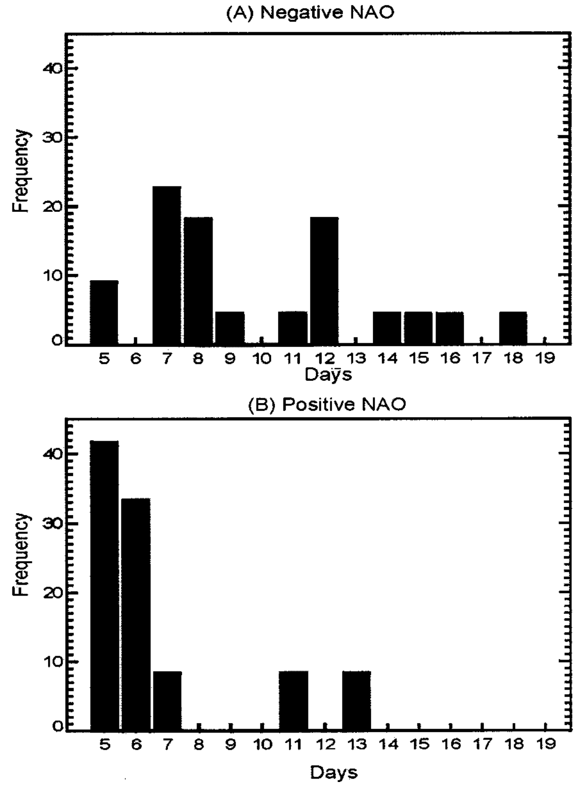

Figure 5. Frequency distribution of blocking duration longer than five days in the Atlantic region for negative and positive NAO

than 6 days. In contrast, during the negative phase of the NAO, only 5% of the blocking lasts less than 6 days and the distribution of blocking duration covers a wide range from 5 to 18 days. The average duration is around 11 days, which is much longer than the duration associated with the positive phase of the NAO (about 6 days). Dole (1989) showed that the development and decay of persistent anomalies in the North Atlantic occur rather rapidly with the de-correlation time of about 10 days. Our analysis of blocking frequency (Figure 5) shows that there is still a significant portion of blocks that have a lifecycle of more than 10 days (some blocks last up to 18 days).

Figure 6 shows a blocking signature pattern in the 500 hPa heights in the North Atlantic region for the negative phase of the NAO. The blocking signature is obtained by subtracting the composite field of all non-blocked days from the composite field of all blocked days (Tibaldi *et al.*, 1997). The map shows the shape, extension and intensity of the mean blocking structure during the negative phase of the NAO. The blocking dipole structure is quite evident over the North Atlantic region. In addition, the dipole structure over eastern Canada with a positive anomaly centre southeast of Greenland, and a negative anomaly centre over Hudson Bay, supports enhanced blocking activity over the Canadian region. The concurrent occurrence of blocking in these two regions suggests that the North Atlantic blocking episodes may influence atmospheric blocking over the Canadian region.

The results presented in this section strongly support a statistical relationship between the negative phase of the NAO structure and enhanced blocking activity in the North Atlantic and the Canadian regions. These observations strongly suggest that the flow regime configuration, i.e. the negative phase of the NAO provides the right conditions for the formation and sustenance of blocking activity in the North Atlantic and that the NAO is not merely the result of blocking activity. A dynamical explanation of how the phases of the NAO effect block formation will be presented in the following section.

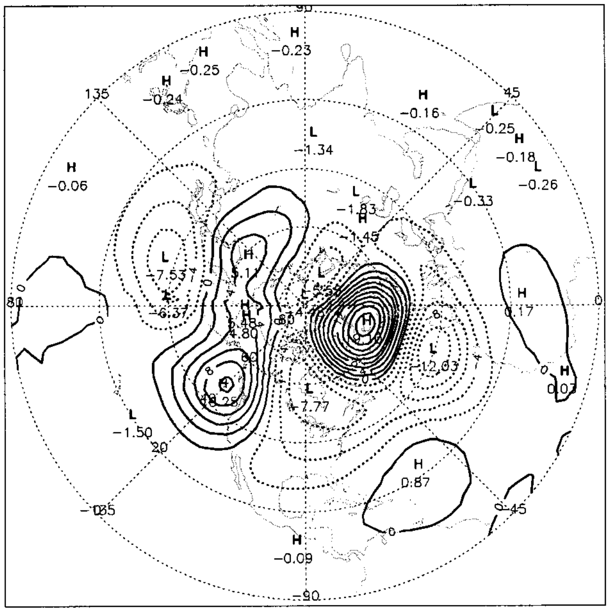

Figure 6. Blocking signature in the 500 hPa heights (i.e. the difference of blocked and zonal climate) of the Atlantic blocking for negative NAO for the period of December–March. Contour interval is 2.0 dams

4. THE IMPACT OF THE NAO ON BLOCKING

To understand the impact of the NAO on blocking, we first need to understand the dynamics of blocking. Although there is not a generally accepted theory for the dynamics of blocking, it has been recognized that non-linear interaction and surface thermal forcing are the two essential factors. Because topography is time invariant, the interannual variability of surface thermal forcing should be related to the interannual variation of blocking. Using a simplified version of Charney and DeVore's (1979) model, we will show the existence of two stable equilibrium states (a low-index flow and a high-index flow). Depending on the zonally asymmetric thermal forcing, the system bifurcates between these equilibrium states. While it may seem intuitive that the negative phase of the NAO would result in more blocking episodes, we will argue that the negative phase of the NAO provides the appropriate thermal forcing which creates an environment conducive for block formation. These theoretical results thus provide a basis for explaining why the blocking frequency and duration in the North Atlantic region are sensitive to the phase of the NAO.

Following Charney and DeVore (1979), the non-dimensional quasi-geostrophic potential vorticity equation with topography and thermal forcing can be written as

$$\frac{\partial}{\partial t}\left(\nabla^2\psi - \frac{\psi}{\lambda^2}\right) + J(\psi, \nabla^2\psi + h) + \beta\frac{\partial\psi}{\partial x} = k\nabla^2(\psi^* - \psi) \tag{3}$$

where ψ is the non-dimensional streamfunction, h is the non-dimensional topographic elevation, ∇^2 is the horizontal Laplace operator, J is the Jacobian operator, $\beta = L/a \cot \phi_0$, ϕ_0 is the central latitude, a is the radius of the earth, $k = D_E/2H$, D_E is the Ekman depth and H the equivalent depth of the atmosphere and ψ^* is the non-dimensional equivalent thermal forcing.

We expand ψ, ψ^* and h in orthonormal eigenfunction of the Laplace operator. To simplify the problem, we keep only those terms that are of direct relevance to the dynamics of the blocking situation being examined in this study and truncate at three functions, instead of the six functions used by Charney and DeVore (1979). The three functions are:

$$F_A = \sqrt{2}\cos y, \quad F_K = 2\cos nx \sin y, \quad F_L = 2\sin nx \sin y$$

where the function F_A allows a zonal flow solution, while the wave functions F_K and F_L permit asymmetric forcing at the bottom boundary of the model. Setting

$$\psi = \psi_A F_A + \psi_K F_K + \psi_L F_L$$
$$\psi^* = \psi_A^* F_A + \psi_K^* F_K$$
$$h = \frac{h_0}{2H} F_K$$

we obtain

$$\dot{\psi}_A = -k(\psi_A - \psi_A^*) + h_{01}\psi_L \quad (4)$$
$$\dot{\psi}_K = -(\alpha_{n1}\psi_A - \beta_{n1})\psi_L - k(\psi_K - \psi_K^*) \quad (5)$$
$$\dot{\psi}_L = -(\alpha_{n1}\psi_A - \beta_{n1})\psi_K - k(\psi_K - h_{n1})\psi_A \quad (6)$$

where

$$\gamma_{n1} = \frac{8\sqrt{2}}{3\pi} n, \quad h_{01} = \gamma_{n1}\frac{h_0}{2H}, \quad h_{n1} = \frac{\gamma_{n1}}{n^2+1}\frac{h_0}{2H}, \quad \alpha_{n1} = \frac{n^2}{n^2+1}\gamma_{n1} \quad \text{and} \quad \beta_{n1} = \frac{n}{n^2+1}\beta$$

Solving for the equilibrium solution of the system of differential equations given by Equations (4)–(6), we arrive at the following equation in $\overline{\psi_A}$ (hereafter the overbar will denote an equilibrium)

$$\overline{\psi_A^3} + v_1\overline{\psi_A^2} + v_2\overline{\psi_A} + v_3 = 0 \quad (7)$$

where

$$v_1 = -(2\beta_{n1}\alpha_{n1} + \alpha_{n1}^2\psi_A^*)/\alpha_{n1}^2,$$
$$v_2 = (\beta_{n1}^2 + k^2 + 2\beta_{n1}\alpha_{n1}\psi_A^* + h_{01}(h_{n1} - \alpha_{n1}\psi_K^*))/\alpha_{n1}^2$$

and

$$v_3 = ((\beta_{n1}^2 + k^2)\psi_A^* + h_{01}\beta_{n1}\psi_K^*)/\alpha_{n1}^2$$

The polynomial form (7) of the equilibrium equation shows that we can, at most, have three equilibria for certain values of the forcing parameters. The stability of an equilibrium solution is determined from the characteristic values of the third order coefficient matrix of the linear perturbation equation resulting from Equations (4)–(6) (Charney and DeVore, 1979).

The equilibrium bifurcation associated with the changes to the parameter of zonally asymmetric thermal forcing ψ_K^* for $k = 2*10^{-2}$, $h_0/H = 0.05$, $n = 2$, $\psi_A^* = 0.2$ is shown in Figure 7. When the asymmetric heating

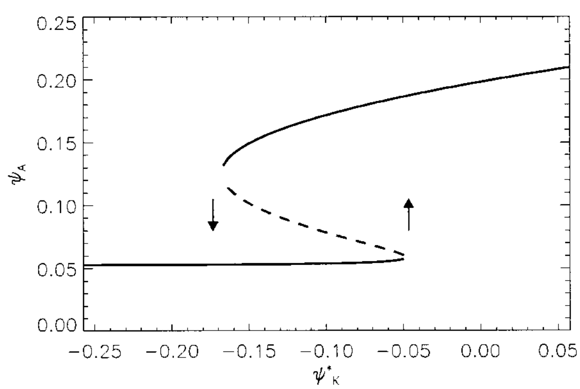

Figure 7. The equilibrium bifurcation associated with the changes in the parameter of zonally asymmetric thermal forcing. The ordinate gives the values of equilibrium $\overline{\psi_A}$. The abscissa gives the parameters of zonally asymmetric thermal forcing ψ_K^*. Parameter values are: $k = 2*10^{-2}$, $h_0/H = 0.05$, $n = 2$, $\psi_A^* = 0.2$

is weak or cooling over the ocean and heating over land (i.e. $\psi_K^* > -0.05$), the large-scale flow has only one possible equilibrium state which is predominated by the zonal component due to the large value of $\overline{\psi_A}$. A numerical evaluation of the corresponding eigenvalues has shown that this equilibrium is always stable.

With increasing heating over oceans and cooling over land areas ($-0.17 < \psi_A^* < -0.05$), a change from a state of one stable solution to a state of two stable and one unstable equilibrium solutions occurs. The unstable regime is indicated by the dashed curve in Figure 7. In this case, the atmosphere is driven into one of the two stable and totally different flow types, one zonal and the other meridional. Which stable flow regime the atmosphere is attracted to is crucially dependent on the initial state of the flow and the way in which the surface thermal forcing changes in time. Once the atmosphere has reached the 'attractor basin' of one of the stable states, it stays there until the forcing changes to drive it away into some other attractor basin. When the asymmetric thermal forcing is characterized by strong heating over the ocean and cooling over land (i.e. $\psi_K^* < -0.17$), the large-scale flow has only one possible equilibrium state which is predominated by wave component.

The two stable equilibrium solutions for a wintertime type thermal forcing pattern of relatively warm ocean/cold land ($\psi_K^* = -0.1$) are shown in Figure 8. The meridional flow regime with a pronounced wave component (Figure 8(A)) may be associated with a 'blocked' situation, while the flow regime shown in Figure 8(B) is related more to a zonal circulation (Charney and DeVore, 1979). Although the model, which is basically conceptual in nature, cannot reveal such an aspect of a blocking situation as the localized dipole structure observed over the North Atlantic (Figure 6), the model, as simple as it is, does demonstrate that a zonally asymmetric thermal forcing is an essential dynamical factor in determining the type of large-scale atmospheric flow.

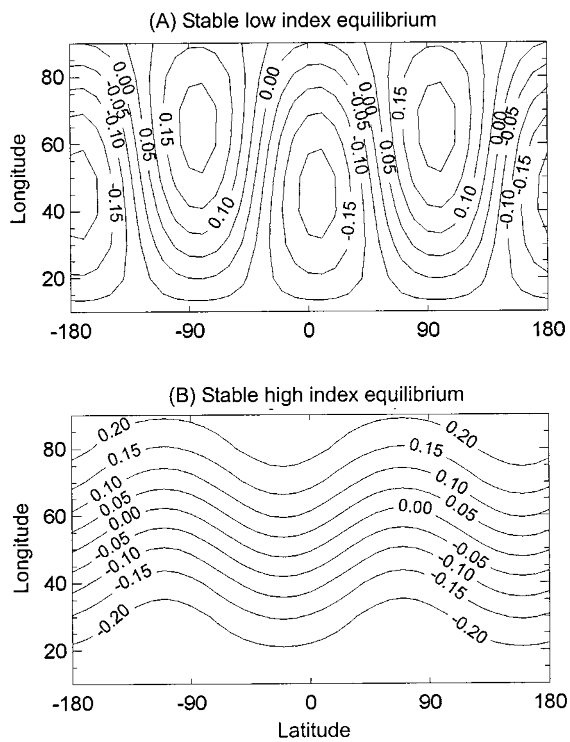

Figure 8. Streamfunction fields of the two stable equilibria for $\psi_K^* = -0.1$ in Figure 7 for stable low and high index equilibria

We have, so far, established a significant statistical relationship between the phases of the NAO and blocking over the North Atlantic. We have also provided, using a simpler version of the Charney/DeVore theoretical model, a dynamical basis for the possibility of occurrences (and non-occurrences) of atmospheric blocks. We will now proceed to present a statistical relationship between the thermal forcing pattern needed for a blocking situation (required by the Charney/DeVore model) and the phases of the NAO, and to argue, based on existing evidence, that the negative phase of the NAO is an influential factor in causing the thermal forcing pattern conducive to the formation of a block in the North Atlantic. In order to explore the relationship between the NAO and the configuration of surface thermal forcing, we compare the composite wintertime surface air temperature anomalies (SATA) associated with the two phases of the NAO, as shown in Plate 1. For the negative phase of the NAO, the distribution of the SATA shows a general but distinctive 'warm ocean/cold land' pattern across the mid and high latitudes of the North Atlantic basin (Plate 1(A)). The pattern is, of course, not theoretically ideal in its configuration, but the warming is centred over the Baffin Bay/Labrador Sea and the western North Atlantic. In this case, where the surface thermal forcing pattern is associated with the negative NAO, the zonally asymmetric thermal forcing and topographic forcing are basically in phase, i.e. heating over ocean and cooling over land. The thermal forcing acts in concert with the resonance forcing of the topography and in accordance with the Charney/DeVore model produces an environment favourable for the formation and persistence of blocking. For the positive phase of the NAO, the distribution of the SATA anomalies reflects the 'cold ocean/warm land (COWL)' pattern (Plate 1(B)) which is almost diametrically opposite to the teleconnection pattern associated with the negative phase of the NAO. In this case, the zonally asymmetric thermal and topographic forcings are out-of-phase, i.e. cooling over ocean and heating over land. The thermal forcing reduces or destroys the resonance forcing of the topography, making block formation difficult, though not impossible.

Now the question arises as to whether the NAO causes the associated changes in the SATA pattern, as seen in Plate 1. We believe that it is possible. Although there are studies which indicate that 'North Atlantic sea surface temperatures (SSTs) do force the NAO on a longer than interannual timescale' (Rodwell *et al*., 1999), several investigators have already demonstrated that the surface temperature anomaly pattern over the North Atlantic and adjacent land areas is determined by the phase of the NAO (Nesterov, 1992, 1998). Nesterov (1992) demonstrated that the NAO plays 'a major role in the formation of the ocean thermal regime' and that the SST anomalies in the northwestern North Atlantic lag the atmospheric pressure anomalies there by about a month. Also, the anomalous coldness over the past decade near Greenland and the eastern Mediterranean and the very warm conditions over Scandinavia, northern Europe and the former Soviet Union are strongly related to the persistent and exceptionally strong positive phase of the NAO index since the early 1980s (Hurrell, 1995; see also Plate 1(B)). Using a multivariate linear regression analysis, Hurrell (1996) showed that nearly all of the cooling in the northwest North Atlantic and the warming across Europe and Eurasia since the mid-1970s have resulted from the changes in the NAO, with the NAO accounting for roughly one-third of the hemispheric interannual variance over the past 60 winters. By performing an EOF analysis of wintertime sea-level pressure field over the Northern Hemisphere, Thompson and Wallace (1998) found an annular mode that is strongly coupled to surface air temperature fluctuation over the Eurasian continent. It resembles the more regionalized NAO in many respects, but its primary centre of action covers more of the Arctic, giving it a more zonally symmetric appearance. They refer to it as the Arctic Oscillation (AO).

Thompson *et al*. (2000) went on to demonstrate the contribution of the AO to recent wintertime surface air temperature trends. They found that the hemispheric distribution of the SATA trend resembles the distinctive 'COWL' pattern. Also, the AO dominates the wintertime SATA variability over Eurasia, one of the most important centres of action of the COWL pattern and accounts for much of the contribution to the COWL pattern. The AO-related component accounts for about half of the observed wintertime warming trend over Eurasia and about 30% of that over the Northern Hemisphere continents as a whole.

Bjerknes (1964) also found that the ocean responds to atmospheric anomalies on interannual timescales. Kushnir (1994) found a similar relation between the NAO index and SST, as reported by Bjerknes (1964). Cayan (1992), while analysing composites of positive and negative NAO months in winter, showed that

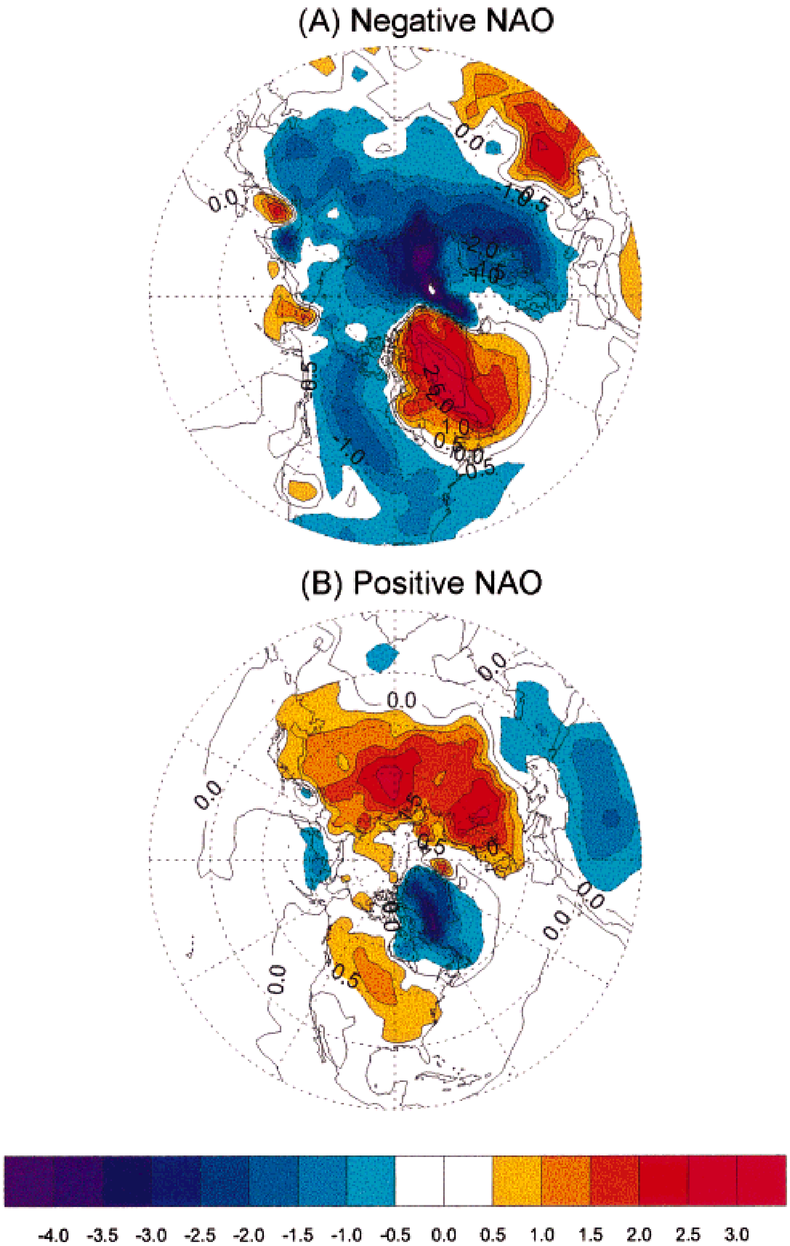

Plate 1. Composite surface air temperature anomaly field of winter (December–March) for negative and positive NAO. Contour intervals in °C

the NAO is responsible for generating systematic large-amplitude patterns in the anomalies of wind speed, latent and sensible heat fluxes and hence sea surface temperature over much of the extra-tropical North Atlantic. It has also been suggested that the interannual and longer-term changes in the winter NAO are an important factor in determining the water temperature and salinity on the West Greenland Banks (Buch, 1995), the temperature and salinity fluctuations in the Greenland and Labrador currents (Reverdin *et al*., 1997) and in controlling temperature anomalies of the western subtropical gyre (Molinari *et al*., 1997). Venegas and Mysak (2000) have shown that, during the negative phase of the NAO, there is an enhanced southward extent of the ice field along the west coast of Greenland. This produces a negative SST anomaly in the Greenland Sea. These results reinforce the role of NAO in determining the configuration of the surface thermal conditions in the North Atlantic region.

5. DISCUSSION AND CONCLUSIONS

The objective of this study was to describe and to gain a deeper understanding of the relationship between the NAO and blocking episodes in the North Atlantic. Although many investigators have examined the NAO and blocking separately, few have explored the statistical and dynamical relationships between them in a unified manner. We have presented strong evidence of a statistical relationship between the negative phase of the NAO and blocking in the North Atlantic sector. By appealing to a simplified version of the Charney and DeVore (1979) theory of blocking, the causal role of the zonally asymmetric nature of the thermal forcing in providing a favourable background environment for block formation was highlighted. In order to unify the relationship between blocking and the NAO, below we offer a dynamical explanation by proposing a conceptual model which links blocking, the NAO and the asymmetric thermal forcing as induced by the land–sea temperature contrast.

Results of the statistical analysis in Section 3 showed that the frequency of blocking formation has significant interannual and interdecadal variability. Further, blocking is strongly related to the phase of the NAO in the North Atlantic region. Seventy five percent more blocking days are observed during wintertime in the negative phase of the NAO compared with those occurring during the positive phase of the oscillation (Figure 3). The lifetime of a blocking episode is also sensitive to the phase of the NAO. When the NAO is in the positive phase, the length of blocking is mainly concentrated near 5–6 days. While in the negative phase of the NAO, the distribution of the length of blocking varies widely. The average length in the negative phase is around 11 days, which is much longer than it is in the positive phase of the NAO (Figure 5). Linear regression analysis reveals that about 30% of the variation in wintertime blocking in the North Atlantic is accounted for by the NAO. Moreover, the unexplainable component of the blocking behaviour does not show a strong trend. This suggests that mechanisms other than the recent warming trend in the climate system may be responsible for this behaviour. In summary, the blocking pattern mainly reflects the superposition of medium scale waves upon a planetary scale background conducive to block formation as exhibited by the existence of the negative phase of the NAO.

Analysis of a low-order theoretical model (Charney and DeVore, 1979) suggests that the NAO-related difference in blocking frequency and persistence are associated with changes in the zonally asymmetric thermal forcing. Numerous observational studies (e.g. Cayan, 1992; Hurrell, 1996, as well as our analysis of the temperature patterns (Plate 1) associated with the different phases of the NAO) show that, on an interannual basis, the NAO modulates the surface temperature anomaly pattern over the North Atlantic and the adjacent landmasses. For the negative phase of the NAO, the distribution of the surface air temperature anomalies is the distinctive 'warm ocean/cold land'' pattern, which enhances the resonance forcing of topography and creates an environment favourable for the formation and persistence of blocking (Plate 1(A) and Figure 8(A)). For the positive phase of the NAO, on the other hand, the distribution of the surface air temperature anomalies is the distinctive 'cold ocean/warm land' pattern, which reduces or destroys the resonant forcing of the topography and is detrimental to blocking formation and persistence (Plate 1(B) and Figure 8(B)).

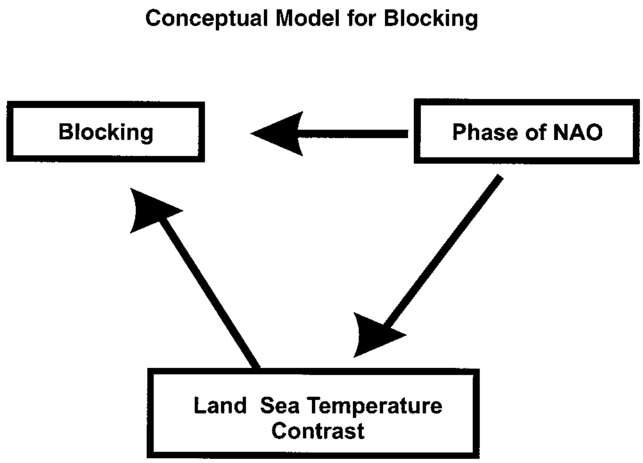

Figure 9. A conceptual model explaining the dynamical link between the NAO and the North Atlantic blocking via the land/sea temperature contrast

Based on the dynamical framework provided by the low-order Charney/DeVore model within which our statistical results linking atmospheric blocking to the phase of the NAO is interpreted, we crystallize these ideas in a conceptual model in which these three components (the NAO, blocking and the thermal contrast between the land and the seas) are interrelated (Figure 9). The dynamical connection between the NAO and blocking can be explained as follows: the phase of the NAO, to a large extent, determines the land–sea temperature distribution over the North Atlantic and the adjacent landmass. As elucidated by the simplified low-order theoretical model, this distribution, in turn, controls the nature of the atmospheric flow, which is either an amplified meridional wave-like flow (favourable for block formation), or a more zonally orientated, i.e. unfavourable for block formation. Thus, a possible physical
mechanism that connects blocking episodes to the phases of the NAO is explained in this model. Blocking events in the North Atlantic do also occur during the positive phase of the NAO; however, they are less frequent and their lifetime is considerably shorter than during the negative phase of the NAO.

The present investigation has revealed several important aspects of the relationship between the NAO and blocking. One of the main shortcomings of our conceptual model is that it does not explain some detailed aspects, such as the localized dipole structure prevalent in blocking events in the North Atlantic. Also, additional analyses and numerical simulations are needed so that the impact of blocking on the NAO and the feedback processes between the two phenomena can be fully understood, to explain, for example, why blocking also occurs during the positive phase of the NAO and why they do not last as long as when they form during the negative phase of the NAO.

ACKNOWLEDGEMENTS

The authors wish to gratefully acknowledge thoughtful comments from an anonymous reviewer.

REFERENCES

Barnston AG, Livezey RE. 1987. Classification, seasonality and persistence of low-frequency atmospheric circulation patterns. *Monthly Weather Review* **115**: 1083–1126.

Bjerknes J. 1964. Atlantic air–sea interaction. In *Advances in Geophysics*, Landsberg HE, Mieghem JV (eds). Academic: San Diego, CA; 1–82.

Buch E. 1995. A monograph on the physical oceanography of the Greenland water. Royal Danish Administration of the Naval and Hydrogological, Copenhagen.

Cayan DR. 1992. Latent and sensible heat flux anomalies over the northern oceans: the connection to monthly atmospheric circulation. *Journal of Climate* **5**: 354–369.

Charney J, DeVore J. 1979. Multiple flow equilibria in the atmosphere and blocking. *Journal of Atmospheric Science* **36**: 1205–1216.

D'Andrea F, Tibaldi S, Blackburn M, Boer G, Deque M, Dix MR, Dugas B, Ferranti L, Iwasaki T, Kitoh A, Pope V, Randall D, Roeckner E, Struas D, Stern W, Van den Dool H, Williamson D. 1998. Northern Hemisphere atmospheric blocking as simulated by 15 atmospheric general circulation models in the period 1979–1988. *Climate Dynamics* **14**: 385–407.

Dole RM. 1989. Life cycles of persistent anomalies. Part I: Evolution of 500 mb height field. *Monthly Weather Review* **117**: 177–211.

Egger J. 1978. Dynamics of blocking heights. *Journal of Atmospheric Science* **35**: 1788–1801.

Hurrell JW. 1995. Decadal trends in the North Atlantic Oscillation: regional temperatures and precipitation. *Science* **269**: 676–679.

Hurrell JW. 1996. Influence of variations in extratropical wintertime teleconnections on Northern Hemisphere temperature. *Geophysical Research Letters* **23**: 665–668.

Hurrell JW, van Loon H. 1997. Decadal variations in climate associated with the North Atlantic Oscillation. *Climate Change* **36**: 301–326.

Kaas E, Branstator G. 1993. The relationship between zonal index and blocking activity. *Journal of Atmospheric Science* **50**: 3061–3077.

Källén E. 1981. The nonlinear effects of orographic and momentum forcing in a low-order barotropic model. *Journal of Atmosphere Science* **38**: 2150–2163.

Kalnay E, Kanamitsu M, Kistler R, Collins W, Deaven D, Gandin L, Iredell M, Saha S, White G, Woollen J, Zhu Y, Chelliah M, Ebisuzaki W, Higgins W, Janowiak J, Mo KC, Ropelewski C, Wang J, Leetmaa A, Reynolds R, Jenne R, Joseph D. 1996. The NCEP/NCAR 40-year reanalysis project. *Bulletin of the American Meteorological Society* **77**: 437–471.

Knox JL, Hay JE. 1984. Blocking signatures in the Northern Hemisphere: rational and identification. *Atmosphere–Ocean* **22**(1): 36–47.

Knox JL, Hay JE. 1985. Blocking signatures in the Northern Hemisphere: frequency distribution and interpretation. *Journal of Climatology* **5**: 1–16.

Kushnir Y. 1994. Interdecadal variations in North Atlantic sea surface temperature and associated atmospheric conditions. *Journal of Climate* **7**: 142–157.

Lejenäs H, Økland H. 1983. Characteristics of Northern Hemisphere blocking as determined from a long time series of observational data. *Tellus* **35A**: 350–362.

Molinari RL, Mayer DA, Festa JF, Bezdek HF. 1997. Multiyear variability in the near-surface temperature structure of the midlatitude western North Atlantic Ocean. *Journal of Geophysical Research* **102**: 3267–3278.

Namias J. 1958. Synoptic and climatological problems associated with the general circulation of the Arctic. *Transactions of the American Geophysical Union* **39**(1): 45.

Nesterov ES. 1992. Influence of the North Atlantic Oscillation on the sea surface temperature. *Soviet Meteorology and Hydrology* **5**: 46–50.

Nesterov ES. 1998. Characteristic features of ocean and atmosphere in different phases of the North Atlantic Oscillation. *Russian Meteorology and Hydrology* **8**: 58–65.

Rex DP. 1950. Blocking action in the middle troposphere and its effect upon regional climate (II). The climatology of blocking actions. *Tellus* **2**: 275–301.

Reverdin G, Cayan DR, Kushnir Y. 1997. Decadal variability of hydrography in the upper northern North Atlantic 1948–1990. *Journal of Geophysical Research* **102**: 8505–8531.

Rodwell MJ, Rowell DP, Folland CK. 1999. Oceanic forcing of the wintertime North Atlantic Oscillation and European climate. *Nature* **398**: 320–323.

Rogers JC. 1984. The association between the North Atlantic Oscillation and the Southern Oscillation in the Northern Hemisphere. *Monthly Weather Review* **112**: 1999–2015.

Shukla J, Mo KC. 1983. Seasonal and geographical variation of blocking. *Monthly Weather Review* **111**: 388–402.

Thompson DW, Wallace JM. 1998. The Arctic Oscillation signature in the wintertime geopotential height and temperature fields. *Geophysical Research Letters* **25**: 1297–1300.

Thompson DW, Wallace JM, Hegerl GC. 2000. Annular modes in the extratropical circulation. Part II: Trends. *Journal of Climate* **13**: 1018–1036.

Tibaldi S, Molteni F. 1990. On the operational predictability of blocking. *Tellus* **42A**: 343–365.

Tibaldi S, D'Andrea F, Tosi E, Roeckner E. 1997. Climatology of Northern Hemisphere blocking in the ECHAM model. *Climate Dynamics* **13**: 649–666.

Tracton MS. 1990. Predictability and its relationship to scale interaction processes in blocking. *Monthly Weather Review* **118**: 1666–1695.

Treidl RA, Birch EC, Sajecki P. 1981. Blocking in the Northern Hemisphere: a climatological study. *Atmosphere–Ocean* **19**: 1–23.

Tung KK, Lindzen RS. 1979. A theory of stationary wave. Part I: a simple theory of blocking. *Monthly Weather Review* **107**: 714–734.

van Loon H, Rogers JC. 1978a. The seesaw in winter tempertures between Greenland and northern Europe. Part I: general description. *Monthly Weather Review* **106**: 296–310.

van Loon H, Rogers JC. 1978b. The Southern Oscillation. Part II: associations with changes in the middle troposphere in the northern winter. *Monthly Weather Review* **109**: 1163–1168.

Venegas S, Mysak L. 2000. Is there a dominant timescale of natural climate variability in the Arctic? *Journal of Climate* **13**: 3412–3434.

Walker GT, Bliss EW. 1932. World weather V. *Memoirs of the Royal Meteorological Society* **4**: 53–84.

Wallace JM, Gutzler DS. 1981. Teleconnections in the geopotential height field during the Northern Hemisphere winter. *Monthly Weather Review* **109**: 784–812.

